Mathematical Modelling and Analysis
Volume 11 Number 3, 2006, pages 295–314
 ISSN 1392-6292 print, ISSN 1648-3510 online

MATHEMATICAL MODELLING DRIVEN BY TWO INDUSTRIAL APPLICATIONS: A MOVING-BOUNDARY APPROACH

A. NARIMANYAN and A. MUNTEAN

Department of Mathematics and Computer Sciences, FB3, University of Bremen, Center for Industrial Mathematics (ZeTeM)

P.O. 330440, D-28334 Bremen, Germany

E-mail: arsen@math.uni-bremen.de; muntean@math.uni-bremen.de

Received March 24, 2006; revised June 26, 2006; published online September 15, 2006

Abstract. This note emphasizes the application of the moving-boundary methodology in the modelling of two processes of particular industrial relevance. The first model explains the application of the Stefan and Signorini type boundary conditions in the modelling of the thermal cutting of metals by a plasma beam, while the second model shows how interface kinetic conditions, employed within the framework of a two-phase Stefan-like model, can describe the dynamics of an aggressive reaction front in concrete-based materials. Our formulations provide a conceptually new approach towards the understanding of the involved physical processes. The connection between the two models is discussed as well. It relies on the presence of non-equilibrium conditions driving the moving interface.

Key words: plasma cutting, concrete carbonation, moving boundaries, Stefan-Signorini boundary condition, interface kinetics, mathematical modelling

1. Introduction

In the practice of mathematical modelling, the study of moving-boundary problems occupies a significant position, mainly because of the importance which it assumes for various questions in the modelling and numerical simulation of several real-world problems. In this work, we present two different phenomena modelled via a moving-boundary approach.

Our first model (see Section 2) is dealing with a thermal cutting process using a plasma beam, while the second one (see Section 3) is concerned with the carbonation of concrete. We develop a new model including physical and mathematical modelling of thermal plasma cutting, which may serve as an important tool for understanding the observable industrial problems. We model

these problems by employing the homogeneous heat-conduction equation accompanied with Signorini-type boundary conditions for the computation of temperature distribution in the workpiece and Stefan-type boundary condition for describing the evolution of the geometry of cutting front. Afterwards, we report on a conceptually new way of modelling the carbonation penetration in concrete-based materials. The resulting model consists of a two-phase moving-boundary system of parabolic partial differential equations coupled with a non-local differential equation which drives the motion of the reaction front. The final aim is twofold:

(a) we want to contribute to the basic understanding of the complex dynamics of a fast reaction in non-saturated reactive porous media;

(b) we intend to formulate a complete model which allows the simultaneous determination of the position of the reaction front and of the fields of the active concentrations.

The results contained in sections 2 and 3 have been partially reported in [25] and [21], respectively. We conclude the paper with a discussion on the connection of the two given problems.

2. Problem 1: Mathematical Modelling of Thermal Cutting

2.1. Problem statement

There is a wide range of thermal cutting techniques available for the shaping of materials. One example is the *plasma cutting*. The origin of the plasma-arc process goes back to 1941. In an effort to improve the joining of light metals for the production of aircraft, a new method of welding was born that used an electric arc to melt the material and a shield of inert gas around the electric arc to protect the molten metal from oxidation. Figure 1(a) [1] gives an impression on some typical applications of plasma cutting.

The essential idea of cutting is to focus a lot of power onto a small area of surface of the material producing intense surface heating. First the material on the surface melts and then evaporates. As the vapour is puffed away or the molten metal is removed by the high speed gas flow, so a hole develops in the material. As the plasma cutting advances by melting, a characteristic feature is the greater degree of melting towards the top of the workpiece resulting in top edge rounding and poor edge squareness. Top edge rounding is a slight rounding of the metal along the top edge of the cut and it is mostly effected by material thickness. This effect is more apparent in thinner metals. The poor edge squareness causes additional difficulties on the next step in the manufacturing process (see Figure 1(b)). If the cut piece has to be welded, a high quality cut with square edges is especially important for the integrity of the weld.

[1] Pictures are taken from www.torchmate.com/automate/cncdemo.html and www.rtgstore.com/art

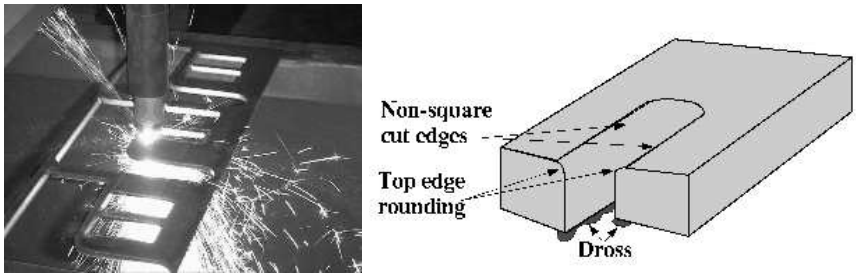

(a) (b)

Figure 1. (a) An applications of plasma cutting. (b) Some typical industrial problems.

One of the characteristics of the cut is the speed with which the plasma jet moves with respect to the workpiece. This speed is the main responsible for another problem in industry, namely, dross formation, see figure 1(b) and [26] for detailed discussions.

Investigations are needed for the prediction and control of the above mentioned phenomena concerning the plasma arc cutting process. To get a quantitative description of the process, one requires a mathematical model for it. It must involve the different physical phenomena occurring in the workpiece during the cut, i.e. heat conduction, convection and radiation effects, mechanical deformations, phase transition, etc. The model has then to be numerically simulated, and the results of the simulations have to be verified by experiments. We do not cope with these issues here and refer the reader to [25].

2.2. Mathematical modelling

There is a vast number of scientific publications concerning the different aspects of mathematical modelling of thermal cutting. In his pioneering work [31] on the mathematical theory of heat distribution during welding and cutting, Rosenthal outlines the fundamentals of the theory and derives analytical solutions for linear two- and three-dimensional flow of heat in solids. In their paper [9] Friedman and Jiang formulated the melting problem of an one-dimensional slab as a Stefan problem with Signorini boundary conditions at the moving boundary. Thereby they established existence and uniqueness theorems for the solution of the problem as well as studied the regularity and some geometric features of the free boundary. In [40] Bui An Ton considered Stefan-Signorini problem with set-valued mappings in bounded domains where he imposed intersecting fixed and free boundary conditions. He proved the existence of a weak solution of Stefan-Signorini problem and showed the continuity of the moving interface. For further readings we refer to [9, 13, 15, 19, 36, 37, 39, 40].

Let consider a high-power plasma beam striking a small area of metal surface. Figure 2 provides a schematic illustration of the plasma cutting process. It shows the plasma beam penetrating through the workpiece, the advancing

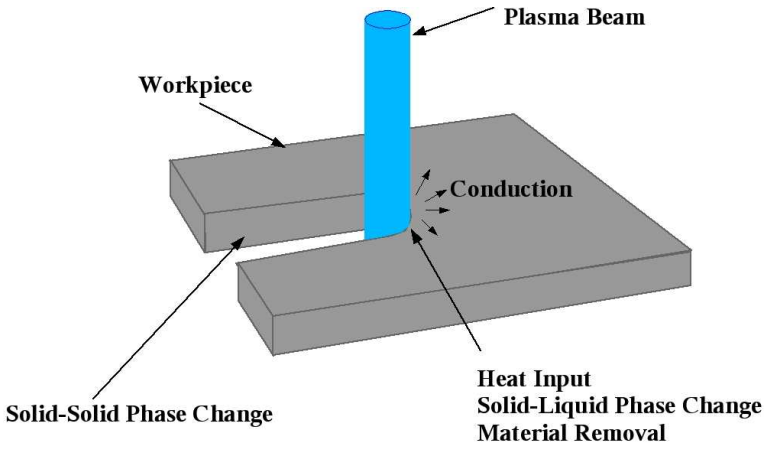

Figure 2. Schematic picture of thermal cutting.

hole and different physical phenomena taking place in the material. The first phenomenon we can observe is the absorption of the energy by the material. The absorption takes place within a thickness usually much less than a millimeter, so we can consider surface heating only. The temperature of the material surface does not rise infinitely. Part of the heat input from the plasma beam melts the metal resulting in solid-liquid phase change in the areas close to the source. When a material melts, latent heat is absorbed without any further rise in temperature. The second part of the heat is transfered into the workpiece by conduction from hotter to colder metal resulting in rise of the temperature in the material. Another physical process is due to the fact that the plasma beam pierces through the workpiece with some constant velocity, while the high velocity gas flow removes the molten material from the bottom of the cut, or the kerf. We do not take into account the effects of the solid-solid phase change, but this can be included in the model by adding supplementary equations describing the phase change in the material. Some earlier publications by A. Schmidt *et al.* [34, 35] and works cited therein are good references on the matter.

Before we present the mathematical model, several modelling assumptions need to be taken into account. Assumptions are made as follows:

- The workpiece is homogeneous and isotropic;
- The material parameters (density, heat capacity, conductivity, etc.) of the workpiece are constant;
- If the piece is large, then the heat exchange through the surface to the surrounding can be neglected with respect to the heat flow in the material itself. This assumption makes sense because the heat conductivity of metals is much greater than the heat transmission through the surface;
- The plasma beam has a cylindrical shape, and the heat flux from the plasma beam is emitted only in the normal direction to the surface of the cylinder.

- The plasma device moves at a constant velocity with respect to the workpiece;
- The heat flux density emitted by the plasma beam is constant and given;
- The heat lost by radiation is negligible;
- The effects of gravity and surface tension are negligible;
- We neglect the thermal and mechanical effects caused by solid-solid phase changes;
- We do not consider the side effects caused by the smoke of the vaporizing metal. By side effects we mean that, for example, the evaporated material does not interfere with the incident plasma beam.

Now we state the assumptions that are necessary to consider in order to give sense to our model. Let Ω be an open and bounded domain in $\mathbb{R}^n$, $n = 2, 3$, occupied by the workpiece. The boundary $\partial\Omega$ of the domain is assumed to be of class $\mathbb{C}^{0,1}$. Let $0 < T < +\infty$ be given, denote by $\theta(x,t)$ the temperature of the workpiece and I the time interval $(0,T)$. The initial temperature distribution of the workpiece is given by $\theta_0(x)$, which is less than the melting temperature at all points. For every $t \in I$ the domain Ω is assumed to consist of two non-intersecting parts, namely $\overline{\Omega} = \overline{\Omega_s(t)} \cup \overline{\Omega_c(t)}$, where $\Omega_s(t)$ and $\Omega_c(t)$ are the domains occupied by the solid part of the workpiece and cut cavity at a time instant t, respectively. Let $\partial\Omega_s(t)$ be the boundary of the time dependent domain $\Omega_s(t)$ at time t (free interface)and we assume that $\partial\Omega_s(t)$ is also a smooth curve. By ν we denote the unit outward normal vector of the domain $\Omega_s(t)$. Let j_{abs} be the heat flux density (heat flux per unit surface) absorbed by the melting interface due to the plasma beam radiation. In addition to the terms defined above we use the following notations: ρ is the density of the workpiece, c_s is the specific heat, k is the heat conductivity of the material, L_m is the latent heat of melting, θ_m is the melting temperature, $v \geq 0$ is the velocity of the melting front.

Assuming that no heat exchange can happen between the workpiece and the exterior through $\partial\Omega_s(t)$, the mathematical model governing the cutting process is the following:

Problem 1. Find the function $\theta(x,t) \in \mathbb{C}_1^2(\Omega_s \times I) \cap \mathbb{C}(\overline{\Omega_s \times I})$, representing the temperature of the body, and the piecewise smooth surface $\partial\Omega_s(t)$ representing the free boundary of the solid domain $\Omega_s(t) = \{x;\ \theta(x,t) < \theta_m\}$, such that the heat conduction equation is fulfilled

$$\rho c_s \frac{\partial\theta}{\partial t} = \nabla \cdot (k\nabla\theta), \quad x \in \Omega_s(t), \quad t \in I, \tag{2.1}$$

with the following boundary conditions on $\partial\Omega_s(t)$:

$$\begin{aligned} &\theta \leq \theta_m, \quad j_{abs} - k\nabla\theta \cdot \nu \geq 0, \\ &(\theta - \theta_m)(j_{abs} - k\nabla\theta \cdot \nu) = 0, \end{aligned} \tag{2.2}$$

called the *Signorini-type* boundary conditions and

$$k\nabla\theta \cdot \nu - \rho L_m v \cdot \nu = j_{abs}, \tag{2.3}$$

named the *Stefan-type* boundary condition. As for the initial conditions, we set

$$\theta(x,0) = \theta_0(x) < \theta_m, \quad x \in \Omega, \quad \Omega_s(0) = \Omega. \tag{2.4}$$

In the following we discuss the boundary conditions (2.2) by considering two sets of points on the boundary $\partial\Omega_s(t)$:

1. Select all points x on the boundary, for which the condition

$$\theta(x,t) < \theta_m \tag{2.5}$$

holds, i.e. the temperature on some part of the boundary is less than the melting temperature. Cut edges behind the plasma jet or boundary surface, where no direct heat input takes place, are two sets of boundary points at which the strict inequality (2.5) is satisfied. At these points of the material the surface absorbs energy coming from the heat source and completely conducts it into the workpiece. As a result, surface heating takes place. The condition of complete conduction can be written as

$$j_{abs} - k\nabla\theta \cdot \nu = 0,$$

meaning that the heat input from the plasma jet is equal to the heat conducted into the material.

2. Select all points x on the boundary, for which the condition

$$\theta(x,t) = \theta_m, \tag{2.6}$$

holds, i.e. the temperature at the points of boundary is equal to the melting temperature. The area of the cut edges very close to the plasma jet is a good candidate for being part of the boundary fulfilling (2.6). The melting of the material takes place on this part of the boundary. The boundary condition for melting can be expressed as

$$j_{abs} - k\nabla\theta \cdot \nu > 0,$$

meaning that the energy input from the heat source is greater than the amount of heat conducted. This is indeed clear, while part of the heat input is used for melting the material (latent heat is absorbed) and only a part of it is conducted.

Summing up both cases, we obtain the following conditions on the boundary of the workpiece

$$\begin{aligned} \theta(x,t) < \theta_m &\Rightarrow j_{abs} - k\nabla\theta \cdot \nu = 0, \\ \theta(x,t) = \theta_m &\Rightarrow j_{abs} - k\nabla\theta \cdot \nu \geq 0, \end{aligned}$$

which yields the Signorini-type boundary conditions (2.2).

The boundary condition (2.3) is referred to as the *Stefan-type condition* and follows from the energy conservation law by its application to elementary volumes that contain both sides of the boundary at the same time. More

precisely, let us consider an element $d\gamma$ of interface that moves with velocity v, and denote by j_{abs} the heat flux (per unit surface) absorbed by the solid boundary and by q_c the heat flux conducted in the solid phase. Latent heat is absorbed at a rate $-\rho L_m v \cdot \nu d\gamma$. The heat exchanged by the interface $\partial\Omega_s(t)$ itself through $d\gamma$ is equal to $(j_{abs} - q_c \cdot \nu)d\gamma$. Applying the energy conservation law to the elementary surface $d\gamma$, we obtain

$$(j_{abs} - q_c \cdot \nu)\, d\gamma = -\rho L_m v \cdot \nu d\gamma \tag{2.7}$$

Dividing both sides of (2.7) by $d\gamma$ and using Fourier's law leads to the *Stefan-type condition* on the moving interface

$$k\nabla\theta \cdot \nu - \rho L_m v \cdot \nu = j_{abs}, \tag{2.8}$$

which is nothing else but the condition (2.3).

Remark 1. The heat flux density j_{abs} and v are equal to zero on the part of boundary where no heat input takes place. Therefore, on that part of the boundary we have homogeneous Neumann conditions.

Remark 2. The idea behind the Stefan-type boundary condition is relatively simple; the total heat flux absorbed by the interface is divided into two parts: one part is conducted and the other part is used to melt the material.

Remark 3. Problem (2.1)–(2.4) could be referred to as an one phase Stefan problem, although there are some important differences between them. The one-phase Stefan problem represents a special case of the classical two-phase formulation, with the temperature being constant in one of the phases, assuming the melting value. Here we have a different situation. First of all, we can not assume the value of the temperature in the cavity (where the melt is removed) equal to the melting temperature of the solid, because otherwise the cut edges will continue to melt and move forward, which does not correspond to the real situation of plasma cutting. Secondly, in our problem an additional heat source (plasma beam) is applied on the surface of the moving front and the heat flux at the interface enters the Stefan type boundary condition which is not the case in classical one-phase Stefan problem.

Note that the Signorini boundary condition is non-linear. At each fixed instant t there exist two regions: in one region we a have heating phase, while in the other a melting phase is present. Moreover, these regions are not prescribed and have to be computed together, resulting in a *moving boundary problem.* The melting front $\partial\Omega_s(t)$ is the unknown moving boundary under consideration.

We call problem (2.1)–(2.4) *the thermal-cutting model* and note that the developed mathematical model is rather general and does not depend on the type of cutting. The main difference between different cuttings is the amount of energy absorbed by the workpiece, which depends on the thermo-physical properties of the material as well as on the several parameters of the heat source. Therefore, the heat flux density j_{abs} is an additional important object

for modelling. A simple way to calculate the flux density at every point of the cutting front is described in [25].

Note that in the model we are mainly concerned with the problem of heat transfer and temperature distribution in the workpiece during the thermal plasma cutting. The problem is solved, if any moment the temperature of every point of the workpiece and the geometry of the workpiece are identified.

Remark 4. **Analysis of the cutting model.** In [33] the weak formulation of the cutting model is derived by rewriting the classical model in terms of variational inequalities and level set method. Analytical results concerning the existence and uniqueness of weak solutions of the model are presented in [25] (see Lemma 6.2.2 and Lemma 6.2.4). In the latter work the author also presents a numerical scheme for solving the cutting problem using the adaptive finite element method. The convergence of the implemented numerical algorithm is obtained as well (see section 7.2 in [25]).

3. Problem 2: Mathematical Modelling of Concrete Carbonation

3.1. Problem statement

It is generally accepted that the steel reinforcement in concrete is protected from corrosion by a passive film formed by the alkali pore solution in contact with the steel bars. Once the alkalinity is altered as a result of carbonation, that is

$$CO_2(g \to aq) + Ca(OH)_2(aq \to s) \to CaCO_3(aq \to s) + H_2O, \qquad (3.1)$$

the environment in concrete at the micro- and meso-scales near the bars becomes corrosive in the presence of pore water and oxygen. We propose a moving-reaction layer model in order to describe the carbonation process based upon (3.1). The corner stones of this approach are the typical pictures of sliced partially carbonated specimens after spraying a pH indicator (e.g. phenolphthalein), see figure 3 (a). Such pictures show a reacted zone separated by a transition-reaction layer from the not reacted part. Having this observation in mind, we intend to identify what determines the progress of the reaction layer into the sample and what penetration speeds can actually be physically permitted. Employing a concept used in the modelling of melting problems (cf. [1, 20, 32], e.g.), this separating layer remotely resembles to a mushy region. In this area connecting the carbonated and uncarbonated parts, the reactants and products may not be segregated.

Specifically, we may consider that the chemistry of the specimen is known and the environmental (boundary) conditions can be perfectly controlled. A correct description of layer's motion contributes to a better prediction of corrosion. The general motivation of such investigation lies in the usual tendency of replacing the transition layer by a moving singular surface where the reaction is supposed to take place. We focus our attention on the solid-solid interfacial

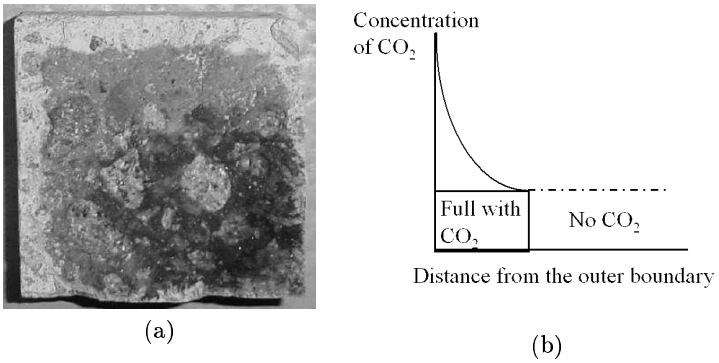

Figure 3. (a) Typical result of the phenolphthalein test on a partially carbonated sample (Courtesy of U. Dahme (AG Setzer), University of Duisburg-Essen, Germany). The dark region shows the uncarbonated part, while the brighter one points out the carbonated part. The two regions are separated by a thin front. (b) Definition of the front position. Note that (a) and (b) are macroscopic pictures.

phenomena that occur between distinct carbonated and non-carbonated parts. The phases are present in the system and are separated one from another by a very thin reaction layer, which we call *inter-phase layer*. On this way, the bulk reactant concentrations are prevented from being abruptly consumed and the model formally receives some more regularity. The reactants rather have a smoother fast variation over the width of the narrow transition reaction zone. A moving-boundary modelling of the carbonation process is particularly motivated by the success demonstrated by alike formulations in the fields of chemical-reaction engineering [10] and geochemistry [27]. Also see [22, 23] (sharp-interface problems), [24] (thin reaction layers or zones). In the case of reactive porous media, we mention [4] (sulfate attack on sewer pipes), hydration of concrete [29], chloride attack [18] and [30] (dissolution reactions), e.g. The classical multi-phase Stefan problem arising in the modelling of freezing and melting scenarios constitutes a well-founded starting point of our modelling, too. See [8, 20, 32], e.g., for basic analytic facts around these issues. Having this classical example in mind, we have formulated the carbonation process within the framework of moving-reaction layer (or interface) problems in [5] and [21]. We also owe some ideas sustaining a moving-boundary modelling of aggressive reactions in the limited-diffusion regime to a note by Brieger and Wittmann [6] and to the book by Ortoleva [27]. An overview of the physical and chemical phenomena appearing when the carbonation reaction occurs in concrete-based materials may be found in the survey papers by Chaussadent [7] and Kropp [16]. The collection of papers [2] provides an overview of contributions, spanning the last decades, to the continuum theories of evolving-phase interfaces and layers in solids. For specific details on the dynamics of two-phase systems given within the framework of continuum thermodynamics or when a sharp interface separating the bulk phases is assumed, see the book by Gurtin [12]. A setting in which instead of the sharp

interface, the bulk fields are divided by a transition layer, may be noticed in [11].

3.2. Geometry. Basic processes. Choice of porosities

We consider a part of a concrete member that is exposed to ingress of gaseous CO_2 and humidity from the environment. Figure 4 shows a typical control volume (box A) in such a structure. We denote by Ω the whole box A (or part of it) for which we model the carbonation process under natural exposure conditions. The typical situation in the process of concrete carbonation can

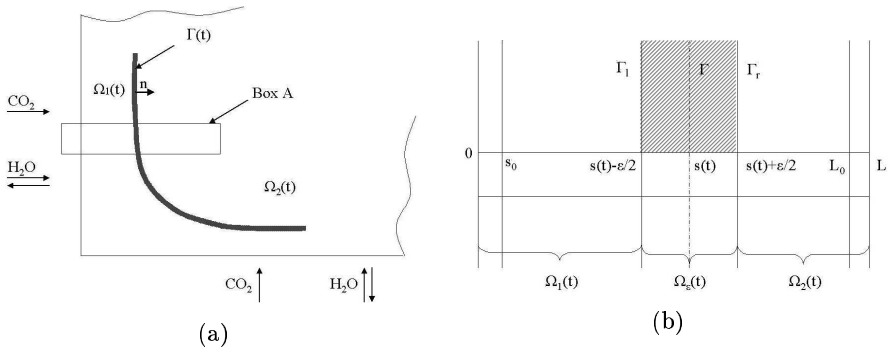

Figure 4. (a) Typical corner of a concrete structure. The box A is the region to which our model refers when dealing with natural exposure conditions. (b) Reaction (3.1) is assumed to happen in $\Omega_\epsilon(t)$ with the reaction rate $\tilde{\eta}_\epsilon$.

be summarised as follows: Generally, the concrete matrix is made of a mixture of water, cement and aggregate. Such mixtures, once they are hardened, have a definite porous structure. The grains (gravel, sand, etc.) have different sizes, hold together by compressing and cementing material and form a multi-phase composite with complex chemistry. To describe reaction-diffusion processes in such multi-phase materials, we make use of a few specific notations and definitions. Let $\Omega(t)$ denote a representative control volume within the concrete sample at the time $t \in S$, where S represents a given time interval. The dependence of Ω on the time t shows that possible changes in the shape and volume could be allowed. The size and shape of this region is assumed to be constant. Therefore, we may account for $\Omega = \Omega(t)$ for all $t \in S$. The region Ω consists of two distinct parts Ω_p and Ω_s. The part Ω_p represents the inner pores space, and Ω_s is the part occupied by the consolidated aggregate and mortar.

We denote by ϕ the volumetric total porosity. By [3, 14], e.g., when Ω_p is the total pore space, regardless of whether the pores are interconnected or not, or whether dead-end pores and fractures are present, the porosity ϕ is referred to as *total* porosity. This quantity is defined as the ratio of volume of the pores space, which we denote by $|\Omega_p|$, and the bulk volume $|\Omega|$ of the

control concrete region. Note also that for most usual cement-based materials (like Ordinary Portland Concrete (OPC), cf. [28]), the porosity $\phi := \frac{|\Omega_p|}{|\Omega|}$ has a value about 0.2. Furthermore, we introduce the notion of material fractions, namely, we define the quantities

$$\phi_a := \frac{|\Omega_a|}{|\Omega_p|}, \quad \phi_w := \frac{|\Omega_w|}{|\Omega_p|}, \quad \phi_s := \frac{|\Omega_s|}{|\Omega|} \tag{3.2}$$

to be the air, water and solid fractions, respectively. In (3.2), $|\Omega_a|$ is the volume of the air-filled parts of the pores space, $|\Omega_w|$ is the volume of the respective water-filled parts and $|\Omega_s|$ denotes the volume of the solid matrix. It holds that

$$\phi_a + \phi_w = 1, \quad \phi\phi_a + \phi\phi_w + \phi_s = 1.$$

Let us now establish a law for the time evolution of the concrete porosity during carbonation, see also [17]. We begin with assuming that

$$\phi = \phi(t) \text{ for all } t \in S. \tag{3.3}$$

Therefore, we restrict our attention to the case for which variations in the space position do not alter the porosity. In the literature, we often find the following ansatz for describing the porosity of a porous medium

$$\phi(t) := \phi_0 e^{-\alpha t}, \tag{3.4}$$

where ϕ_0 is a given initial porosity and α is usually a fitting parameter. In the following we *identify* the meaning of α for a carbonation scenario.

3.2.1. Identification of the parameter α arising in (3.4)

We introduce some auxiliary notation. Let $\mathcal{M}_h$ and $\mathcal{M}_b$ be the molecular weights of $Ca(OH_2)$ and $CaCO_3$. Set ρ_h, ρ_b, h and b to be the densities, and the molar concentrations of $Ca(OH_2)$ and $CaCO_3$, respectively. Note that

$$[\mathcal{M}_E] = g\,mol^{-1}, \quad [\bar{E}] = mol\,cm^{-3}, \quad [\eta] = gcm^{-3}\,day^{-1}, \quad [t] = day.$$

Here E is h and b. Let $\bar{\eta} = \bar{\eta}(x,t)$ be the carbonation reaction rate. Specifically, we have the following proportionality relations $\bar{\eta} \sim a$ and $\bar{\eta} \sim b$.

We argue in the following manner: consider the carbonation process simply described by the replacement mechanism

$$Ca(OH)_2(s) \to CaCO_3(s). \tag{3.5}$$

We assume that at time t_0 there is no carbonation inside $\Omega' \subset \Omega$ and that no calcium carbonates have been yet produced. Thus, it holds

$$\bar{\eta}(x,t_0) = 0, \quad x \in \Omega'.$$

At time t_0, the volume occupied by $Ca(OH_2)$ is $\int_{\Omega'} \frac{h(x,t_0)}{\rho_h}\mathcal{M}_h dx$. To account for the change of the pore structure produced by carbonation, we consider that

in the carbonated region within Ω' the reaction carbonation is *complete*. Let t be an instant at which carbonation happens. The volume occupied by $CaCO_3$ at time t is $\int_{\Omega'} \frac{b(x,t)}{\rho_b}\mathcal{M}_b dx$. We assume that all $Ca(OH)_2$(s) is completely available for reaction via various physiochemical mechanisms. The total content of $Ca(OH)_2(s)$ transforms (by carbonation) into the total content of $CaCO_3(s)$ after a time $t_f - t_0$, if losses of carbonates or of alkaline species via leaching are excluded. The time $t_f - t_0$ can be defined as the time needed to obtain the complete replacement in (3.5). On this way, we expect that the change in porosity is mainly determined by the difference in the densities (or in the molar volumes) of the two species. We introduce the molar contents

$$H(t) := \int_{\Omega'} h(x,t)\,dx, \quad B(t) := \int_{\Omega'} b(x,t)\,dx$$

of the species $Ca(OH)_2$ and $CaCO_3$ at a given time t. If the transport does not affect the reaction, then after a given time $t-t_0$ the content $H(t_0)-H(t)$ of moles of $Ca(OH)_2$ produced the content $B(t)$ of moles of $CaCO_3$. Thus the equality

$$H(t_0) - H(t) = B(t)$$

holds for each $t_0 \le t \le t_f$. Trivially, it also results that $B(t_0) = H(t_f) = 0$. We then have

$$\begin{aligned}\int_{\Omega'} \big(1-\phi(t_0)\big)\,dx - \int_{\Omega'} \big(1-\phi(t)\big)\,dx \qquad (3.6)\\ = \int_{\Omega'} \frac{(h(x,t_0)-h(x,t))}{\rho_h}\mathcal{M}_h\,dx - \int_{\Omega'} \frac{b(x,t)}{\rho_b}\mathcal{M}_b dx\\ = \frac{\mathcal{M}_h}{\rho_h}\left(H(t_0)-H(t)\right) - \frac{\mathcal{M}_b}{\rho_b}B(t) = \left(\frac{\mathcal{M}_h}{\rho_h} - \frac{\mathcal{M}_b}{\rho_b}\right)B(t).\end{aligned}$$

By (3.4) and (3.6), it yields that

$$\phi(t) - \phi(t_0) = \frac{1}{|\Omega'|}\left(\frac{\mathcal{M}_h}{\rho_h} - \frac{\mathcal{M}_b}{\rho_b}\right)B(t), \quad t \in]t_0, t_f]. \qquad (3.7)$$

Denote by β the quantity

$$\beta := \frac{\mathcal{M}_h}{\rho_h} - \frac{\mathcal{M}_b}{\rho_b}. \qquad (3.8)$$

If $\beta > 0$, then the porosity is enhanced. If $\beta < 0$, then the porosity is decreased. For the case of (3.5), we have $\beta = -4.1857$. Hence, a decrease in the concrete porosity induced by (3.5) is to be expected[2]. Furthermore, since b is produced via $\bar{\eta}$, we can write

$$b(x,t) := \int_{t_0}^{t} \phi(\tau)\bar{\eta}(x,\tau)\,d\tau. \qquad (3.9)$$

[2] This fact agrees with the experimental evidence that OPC samples *usually* suffer a decrease in porosity induced by carbonation.

Dividing (3.7) by $\Delta t := t - t_0$ in which $t_0 < t < t_f$ and owing to (3.9), we obtain that

$$\lim_{t \to t_0} \frac{\Delta \phi}{\Delta t} = \frac{\beta}{|\Omega'|} \int_{\Omega'} \lim_{t \to t_0} \frac{1}{\Delta t} \int_{t_0}^{t} \phi(\tau) \bar{\eta}(x, \tau) \, d\tau dx.$$

The latter equation leads to

$$\frac{1}{\phi(t)} \frac{d\phi}{dt} = \frac{\beta}{|\Omega'|} \int_{\Omega'} \bar{\eta}(x, t) \, dx \quad \text{for all} \quad t \in (t_0, t_f). \tag{3.10}$$

Furthermore, if we assume now that

$$0 < \bar{\eta}_{\min} \leq \bar{\eta}(x, t) \leq \bar{\eta}_{\max} < +\infty, \tag{3.11}$$

then by (3.10) and (3.11) the estimates

$$\phi_0 e^{\beta \bar{\eta}_{\max} t} \leq \phi(t) \leq \phi_0 e^{\beta \bar{\eta}_{\min} t} \quad \text{for all} \quad t \in (t_0, t_f)$$

hold. Therefore, possible candidates for α are $\beta \bar{\eta}_{\max}$, $\beta \bar{\eta}_{\min}$, or some mean value, for instance.

Remark 5. (a) If the active concentrations are small, then the constant porosity assumption $\phi := \phi_0$ is valid, see [17], p.164.

(b) If the transformation $Ca(OH)_2(s) \rightarrow Ca(OH)_2(aq)$ can be considered complete and the reverse transformation $Ca(OH)_2(aq) \rightarrow Ca(OH)_2(s)$ has no time to happen, then, as in the case of non-catalytic gas-solid reactions, the total porosity may be assumed to depend linearly on the solid reactant conversion. This translates in our setting as follows: the evolution of the concrete porosity depends linearly on the concentration of $Ca(OH)_2$(aq), or equivalently,

$$\phi := \phi_0 + \bar{h}_0 \frac{\mathfrak{M}_h - \mathfrak{M}_b}{|\Omega|} \left(1 - \frac{\bar{h}}{\bar{h}_0} \right), \tag{3.12}$$

where $\bar{h}_0$ and $\bar{h}$ are molar concentrations of $Ca(OH)_2$(aq) in the points $(x, 0)$ and (x, t), respectively, ϕ_0 is the initial porosity, $\mathfrak{M}_h$ and $\mathfrak{M}_b$ are the reactant and product molar volumes. Here $\mathfrak{M}_h := \mathfrak{M}_{Ca(OH)_2}$ and $\mathfrak{M}_b := \mathfrak{M}_{CaCO_3}$. It can be seen from (3.12) that the porosity ϕ is now a function of x and t. If the product b has a lower molar volume than the reactant h, then the porosity increases, otherwise it decreases.

3.3. Moving reaction layer model

The problem is posed in the time interval $S_T =]0, T[$, $T \in]0, \infty]$ and refers to the geometry described in section 3.2. We select and fix $\epsilon > 0$ sufficiently small, and consider at an arbitrarily given time $t \in S_T$ the domain $\emptyset \neq \Omega \subset \mathbb{R}_+$, i.e. a part of the concrete sample (see [38]), which is divided by the planes $x = s(t) \pm \frac{\epsilon}{2}$ into three distinct sub-domains. At time t the sub-domain $\Omega_1(t) := \Omega \cap \{x < s(t) - \frac{\epsilon}{2}\}$ denotes a partially carbonated part,

while $\Omega_2(t) := \Omega \cap \{x > s(t) + \frac{\epsilon}{2}\}$ represents the uncarbonated part. The third sub-domain is the layer

$$\Omega_\epsilon(t) := \Omega \cap \big\{s(t) - \frac{\epsilon}{2} < x < s(t) + \frac{\epsilon}{2},\ \ t \in S_T\big\},$$

that separates the two regions $\Omega_1(t)$ and $\Omega_2(t)$. Within this layer takes place the bulk[3] of the carbonation reaction. We denote by

$$\Gamma_l(t) := \partial\Omega \cap \big\{x = s(t) - \frac{\epsilon}{2} :\ t \in S_T\big\},\ \ \Gamma_r(t) := \partial\Omega \cap \big\{x = s(t) + \frac{\epsilon}{2} :\ t \in S_T\big\}$$

the planes, which separate these domains, and let the surface $\Gamma(t) := \partial\Omega \cap \{x = s(t), t \in S_T\}$ be located in the middle of the layer, see figure 4. Within this framework, we do not include any surface reaction at $\Gamma_l(t)$, $\Gamma_r(t)$ or $\Gamma(t)$. By Figure 4, we remark a restriction on the choice of ϵ, that is $\epsilon \in (0, L_0 - \mu)$ with $\mu \in (0, L_0)$. For real-world problems, the value of ϵ is sufficiently small, i.e. $\epsilon \ll L_0$. Finally, we have

$$\Omega = \Omega_1(t) \cup \Gamma_l(t) \cup \Omega_\epsilon(t) \cup \Gamma_r(t) \cup \Omega_2(t),$$

or $\Omega = \mathrm{clos}(\Omega_1(\mathrm{t}) \cup \Omega_\epsilon(\mathrm{t})) \cup \Omega_2(\mathrm{t})$. The region $\Omega_2(t)$ can be also defined by

$$\Omega_2(t) := \{x \in \Omega : \phi\phi_w \bar{u}_i(x,t) = 0, i \in \{1,2\}\}, t \in S_T,$$

while $\Omega_1(t) \cup \Omega_\epsilon(t)$ is given by

$$\Omega_1(t) \cup \Omega_\epsilon(t) := \Omega - \Omega_2(t), t \in S_T.$$

We denote the mass concentration of the active species by $\bar{u}_1 := [CO_2(aq)]$, $\bar{u}_2 := [CO_2(g)]$, $\bar{u}_4 := [CaCO_3(aq)]$, $\bar{u}_5 := [H_2O]$ the chemical species present in the domain $\Omega_1(t) \cup \Omega_\epsilon(t)$. Other active species are present in $\Omega_2(t)$, namely $\bar{u}_3 := Ca(OH)_2(aq)$ and $\bar{u}_6 := [H_2O]$. We assume that $CaCO_3$ is not transported in Ω.

The following set of indices is used: $\mathcal{I} := \mathcal{I}_1 \cup \{4\} \cup \mathcal{I}_2$, where the set $\mathcal{I}_1 := \{1,2,5\}$ points out the diffusive active concentrations in $\Omega_1(t)$ and the set $\mathcal{I}_2 := \{3,6\}$ refers to the diffusive active concentrations present in $\Omega_2(t)$. Thus we are led to consider the moving-boundary problem for determining $\bar{u}_i(x,t), i \in \mathcal{I}$ and $s = s(t)$ which satisfy for all $t \in S_T$ the equations

$$\begin{cases} (\phi\phi_w \bar{u}_1)_{,t} - (D_1 \phi\phi_w \bar{u}_{1,x})_x = f_{Henry} - f_{Reac\epsilon},\ \ x \in \Omega_1(t) \cup \Omega_\epsilon(t), \\ (\phi\phi_a \bar{u}_2)_{,t} - (D_2 \phi\phi_a \bar{u}_{2,x})_x = -f_{Henry},\ \ x \in \Omega_1(t) \cup \Omega_\epsilon(t), \\ (\phi\phi_w \bar{u}_3)_{,t} - (D_3 \phi\phi_w \bar{u}_{3,x})_x = f_{Diss} - f_{Reac\epsilon},\ \ x \in \Omega_2(t), \\ (\phi\phi_w \bar{u}_4)_{,t} = f_{Prec} + f_{Reac\epsilon},\quad x \in \Omega_1(t) \cup \Omega_\epsilon(t), \\ (\phi\phi_w \bar{u}_5)_{,t} - (D_5 \phi\phi_w \bar{u}_{5,x})_x = -f_{Reac\epsilon},\ \ x \in \Omega_1(t) \cup \Omega_\epsilon(t), \\ (\phi\phi_w \bar{u}_6)_{,t} - (D_6 \phi\phi_w \bar{u}_{6,x})_x = 0,\ \ x \in \Omega_2(t). \end{cases} \tag{3.13}$$

[3] The domain $\Omega_\epsilon(t)$ is referred to as the *reaction layer*. It is supposed to be the place where the carbonation production term applies.

The initial and boundary conditions are the following

$$\phi\phi_w\nu_{i2}\bar{u}_i(x,0) = \hat{u}_{i0}, \quad i \in \mathcal{I}, \;\; x \in \Omega(0),$$
$$\phi\phi_w\nu_{i2}\bar{u}_i(0,t) = \lambda_i, \quad i \in \mathcal{I}_1, \;\; t \in S_T,$$
$$\bar{u}_{i,x}(L,t) = 0, \quad i \in \mathcal{I}_2, \;\; t \in S_T.$$

The interface and transmission conditions imposed across $\Gamma_r(t)$ are defined in the following way:

$$[j_i \cdot n]_{\Gamma_r(t)} = \theta s'(t)[\phi\phi_w\nu_{i2}\bar{u}_i]_{\Gamma_r(t)}, \quad i \in \mathcal{I}_1 \cup \mathcal{I}_2, \tag{3.14}$$

$$s'(t) = c_s(\epsilon)\frac{\int_{\Omega_\epsilon(t)} \tilde{\eta}_\epsilon(\bar{u}(x,t))dx}{\int_{\Omega_\epsilon(t)} \phi\phi_w\bar{u}_3(x,t)dx}, \quad t \in S_T, \quad s(0) = s_0, \tag{3.15}$$

where

$$\nu_{12} = \nu_{32} := 1, \quad \nu_{22} := \frac{\phi_a}{\phi_w}, \quad \nu_{52} = \nu_{62} := \frac{1}{\phi_w},$$
$$\nu_{i\ell} := 1, \;\; i \in \mathcal{I}, \ell \in \mathcal{I} - \{2\}, \quad j_i := -D_i\nu_{i\ell}\phi\phi_w\bar{u}_i, \;\; i, \ell \in \mathcal{I}_1 \cup \mathcal{I}_2$$

are the corresponding diffusive fluxes, and $\theta \in \{0,1\}$. If $\theta = 1$, condition (3.14) points out a small adsorption term acting at the interface $\Gamma_r(t)$. However, in most of the situations the physical relevant case corresponds to $\theta = 0$. Hence, the whole production by reaction is included in the volume term $f_{Reac\epsilon}$. At $\Gamma_l(t)$ the concentrations and their gradients are continuous and no changes in the model parameters occur. Moreover, we have that $c_s(\epsilon)$, D_i ($i \in \mathcal{I}_1 \cup \mathcal{I}_2$), L and s_0 are strictly positive constants. The boundary data $\lambda_i (i \in \mathcal{I})$ are prescribed in agreement with the environmental conditions to which Ω is exposed. The initial conditions $\hat{u}_{i0} > 0$ ($i \in \mathcal{I}$) are determined by the chemistry of the cement. The concrete porosity $\phi > 0$ and also for the water and air fractions, $\phi_w > 0$ and $\phi_a > 0$, are assumed to be given cf. section 3.2. An important aspect of this model is that we assume the speed of the layer $\Omega_\epsilon(t)$ to satisfy (3.15). However, relation (3.15) is not based on first principles. It is rather an *ad hoc* ansatz that we *a priori* impose to describe the dynamics of the layer $\Omega_\epsilon(t)$. Numerical simulations will show in a further publication that our choice of (3.15) is close to what happens in reality. To define the involved carbonation-reaction rate, we introduce the function

$$\tilde{\eta}_\epsilon : \mathbb{R}^6 \times M_{\Lambda_\epsilon} \to \mathbb{R}_+, \tilde{\eta}_\epsilon(y,t) = \bar{\eta}_\epsilon(\bar{u}(x,t) + \lambda(t), \Lambda_\epsilon), x \in \Omega_\epsilon(t), \tag{3.16}$$
$$\bar{\eta}_\epsilon(\bar{u}(x,t), \Lambda_\epsilon) = k_\epsilon\phi\phi_w\bar{u}_1^{p_\epsilon}(x,t)\bar{u}_3^{q_\epsilon}(x,t), \quad t \in S_T,$$

where $p_\epsilon \geq 1$, $q_\epsilon \geq 1$.

The production terms f_{Henry}, f_{Diss}, f_{Prec} and $f_{Reac\epsilon}$ denote sources and sinks by Henry-like transfer mechanisms, dissolution, precipitation and carbonation reactions. Within this framework, we assume

$$\begin{cases} f_{i,Henry} = (-1)^i P_i(\phi\phi_w \bar{u}_1 - Q_i \phi\phi_a \bar{u}_2),\ P_i, Q_i > 0,\ i \in \{1,2\}, \\ f_{Diss} := -S_{3,diss}(\phi\phi_w \bar{u}_3 - u_{3,eq}),\ \ S_{3,diss} > 0,\ \bar{u}_3 > 0, \\ f_{Prec} := 0, \\ f_{Reac\epsilon} := \tilde{\eta}_\epsilon. \end{cases} \tag{3.17}$$

The reaction layer $\Omega_\epsilon(t)$ is constantly receiving solute reactants from $\Omega_1(t)$ and $\Omega_2(t)$. Also it looses aqueous reaction products and gains precipitated minerals. Thus this moving-reaction zone is manipulated out of equilibrium and generally sustains a host of non-equilibrium phenomena.

Finally, we call the formulation (3.13)-(3.17) the *moving-reaction-layer carbonation model.* This problem consists of a non-local coupled strongly non-linear system of parabolic equations which has a moving *a priori* unknown internal layer. The coupling between the equations and the non-linearities come from the influences of the chemical reaction on the transport part, the porosity ϕ, and from the dependence of the moving regions $\Omega_1(t)$, $\Omega_2(t)$ and $\Omega_\epsilon(t)$ on $s(t)$. Other non-linearities may be introduced by different assumptions on the production terms. The non-locality property stems from equation (3.15) and is essentially related to the dynamics of $\Omega_\epsilon(t)$.

Remark 6. **(Well-posedness of (3.13)-(3.15))** Local and global existence, uniqueness and stability of positive weak solutions with respect to the initial data and parameters are shown in [21] (see Theorem 3.5.4, Theorem 3.5.5 and Theorem 3.5.10). Furthermore, useful upper and lower bounds, for instance on the velocity of the reaction front and on the time to complete the carbonation of a given part of a concrete sample, are also obtained.

4. Discussion on the connection between the two models

Our models for the plasma cutting (Problem 1) and concrete carbonation (Problem 2) are from both mathematical and modelling points of view non standard. They only remotely resemble to the classical Stefan problem of ice melting, which is a standard equilibrium model.

The main aim of the paper has been to show that the moving-boundary methodology can be used in a similar manner for tackling two different real-world problems. In Problem 1 several inequalities govern the evolution of the unknown interface, while in Problem 2 a non-local kinetic condition makes the reaction front to penetrate the concrete. In both situations, *similar interface conditions* drive the involved processes far from equilibrium configurations. This is a major difference with respect to the equilibrium condition defining the Stefan problem, namely the temperature field is continuous when crossing the interface and equal to the melting temperature. The strong non-equilibrium feature intimately connects Problem 1 and Problem 2. It is worth mentioning that the employed modelling strategies, dealing with two real-life problems, can essentially interplay. Instead of imposing unilateral conditions for advancing the cutting front, we could imagine a kinetic law acting as a

driving force. This law refers to the evolution of the normal component of the interface velocity $v \cdot \nu$. It can be obtained for simple geometries via balancing the mass within a shrinking pillbox that contains the moving interface (see Gurtin's Pillbox Lemma [12]). This kind of argument (cf. [21], section 2.3.1) formally yields

$$v \cdot \nu = f(\rho, L_m, j_{abs}, \theta, \chi, \partial\Omega_s(t)),$$

where χ represents the amount of solid component which clings on locally flat parts of the cutting interface and waits to be melt. The precise expression of f is essential for the correctness of the approach.

Now let us see in which way unilateral conditions may play a role when modelling the concrete carbonation. In order to do this, we assume for a moment that the reaction layer $\Omega_\epsilon(t)$ can be replaced by a sharp interface $\Gamma(t)$ and concentrate on the behavior of the most aggressive species (i.e. CO_2(g) or u_1) near $\Gamma(t)$. Firstly, we assume a kinetic condition like

$$s'(t) = \eta_\Gamma(s(t), t),$$

where $s(t)$ is the reference position of the interface $\Gamma(t)$ at time t and η_Γ represents the corresponding surface-reaction rate on $\Gamma(t)$. Instead of the classical form of the Rankine-Hugoniot jump conditions which need to be imposed at $x = s(t)$, we might consider unilateral conditions like

$$\begin{aligned}
&u_1(s(t), t) \geq 0,\\
&-D_1 u_{1,x}(s(t), t) - s'(t) u_1(s(t), t) - \eta_\Gamma(s(t), t) \geq 0,\\
&(s' - \eta_\Gamma(s(t), t))\,(-D_1 u_{1,x}(s(t), t) - s'(t) u_1(s(t), t) - \eta_\Gamma(s(t), t)) = 0.
\end{aligned}$$

The latter relations allow the interface $\Gamma(t)$ to be stationary until sufficient CO_2 arrive at the reaction locus, and therefore, its motion is then allowed to continue. This feature can not be covered by the use of a kinetic condition. Similar inequalities can be enforced for the other active concentrations.

The foregoing discussion has attempted to indicate issues connected with moving boundaries which are driven by two industrial applications. An effort has been made to identify some connection points and create a background where further co-operation between mathematicians and engineers is most desirable.

5. Acknowledgements

The first author thanks the colleagues from Bremen Steel Company for stating the plasma cutting problem in the form described here and, especially, Prof. Dr. A. Schmidt for his invaluable remarks on several issues concerning the study. The work of the second author has been partially supported by a grant through DFG SPP1122. Intensive discussions with Prof. Dr. M. Böhm, Prof. Dr. J. Kropp and Dr. K. Sisomphon on modelling issues concerning concrete carbonation are greatly acknowledged.

The authors are indebted to the referees for their suggestions and for a careful reading of the paper.

References

[1] V. Alexiades and A. D. Solomon. *Mathematical Modelling of Melting and Freezing Processes.* Hemisphere Publishing Group, Washington, Philadelphia, London, 1993.

[2] J. M. Ball, D. Kinderlehrer, P. Podio-Guidugli and M. Slemrod(Eds.). *Evolving Phase Interfaces in Solids.* Springer Verlag, Berlin, 1999.

[3] J. Bear. *Dynamics of Fluids in Porous Media.* Dover Publications Inc., N.Y., 1972.

[4] M. Böhm, J. Devinny, F. Jahani and G. Rosen. On a moving-boundary system modelling corrosion in sewer pipes. *Appl. Math. Comput.*, **92**, 247–269, 1998.

[5] M. Böhm, J. Kropp and A. Muntean. *A two-reaction-zones moving-interface model for predicting $Ca(OH)_2$-carbonation in concrete.* Berichte aus der Technomathematik 03-04, ZeTeM, University of Bremen, 2003.

[6] L. M. Brieger and F. H. Wittmann. Numerical simulation of concrete carbonation. In: F. H. Wittmann(Ed.)(Ed.), *Werkstoffwissenschaften und Bausanierung.* Technische Akademie Esslingen, 635–640, 1986.

[7] T. Chaussadent. États de lieux et réflexions sur la carbonatation du beton armé. Technical report, Laboratoire Central de Ponts et Chaussées, Paris, 1999.

[8] A. Friedman. *Variational Principles and Free-Boundary Problems.* R.E. Krieger Publishing Company, Malabar, Florida, 1988.

[9] A. Friedman and L. Jiang. A Stefan-Signorini problem. *J. Differential Equations*, **51**, 213–231, 1984.

[10] G. F. Froment and K. B. Bischoff. *Chemical reactor analysis and design.* Wiley Series in Chemical Engineering. John Wiley and Sons, NY, Chichester, Brisbane, Toronto, Singapore, 1990. 2nd edition

[11] L. Graziano and A. Marasco. Balance laws for continua with an interface deduced from multiphase continuous models with a transition layer. *Int. J. Engng. Sci.*, **39**, 873–986, 2001.

[12] M. E. Gurtin. *Thermomechanics of Evolving Phase Boundaries in the Plane.* Clarendon Press, Oxford, 1993.

[13] H. Hafercamp, M. Niemeyer, J. Hoerner, J. Bosse, M. Kock and F. Könemann. Numerical modelling of thermal plasma cutting. In: *Thermal cutting conference.* Timisoara, 1999.

[14] R. Helmig. *Multi-Phase Flow and Transport Processes in the Subsurface. A Contribution to the Modelling of Hydrosystems.* Environmental Engineering, Springer Verlag, Berlin, 1997.

[15] M. Kim. Transient evaporative laser-cutting with boundary element method. *Journal of Applied Mathematical Modelling*, **25**, 25–39, 2000.

[16] J. Kropp. Relations between transport characteristics and durability. In: *Performance Criteria for Concrete Durability, RILEM Report*, volume 12, 97–137, 1995. E and FN Spon Editions

[17] J. D. Logan. Transport Modelling in Hydrogeochemical Systems. In: *Interdisciplinary Applied Mathematics.* Springer Verlag, NY, Berlin, 2001.

[18] M. Mainguy and O. Coussy. Propagation fronts during calcium leaching and chloride penetration. *ASCE J. Engng. Mech.*, **3**, 252–257, 2000.

[19] K. Matsuyama. Mathematical modelling of kerf formation phenomena in thermal cutting. *Welding in the World*, **39**(1), 28–34, 1997.

[20] A. M. Meirmanov. The Stefan Problem. In: *De Gruyter Expositions in Mathematics*, volume 3. Walter de Gruyter, Berlin, NY, 1992.

[21] A. Muntean. *A moving-boundary problem: modelling, analysis and simulation of concrete carbonation.* PhD thesis, ZeTeM, Faculty of Mathematics, University of Bremen, 2006. Cuvillier Verlag, Göttingen

[22] A. Muntean and M. Böhm. Dynamics of a moving reaction interface in a concrete wall. In: *Free and Moving Boundary Problems. Theory and Applications, International Series of Numerical Mathematics*, volume 154, Birkhäuser, Basel, 317–326, 2006.

[23] A. Muntean and M. Böhm. Lower bounds on the weak solution of a moving-boundary problem describing the carbonation penetration in concrete. In: *Mathematical Modelling of Environmental and Life Sciences Problems*, Romanian Academy of Sciences, Bucharest, 175–184, 2006.

[24] A. Muntean and M. Böhm. On a moving reaction layer model for the prediction of the service life of concrete structures. In: *Proceedings of the International Conference Performance based Engineering for 21st Century.* Technical University of Iasi, Romania, Cerni Press, Iasi, 72–77, August 2004.

[25] A. Narimanyan. *Stefan-Signorini moving boundary problem arisen from thermal plasma cutting: mathematical modelling, analysis and numerical solution.* PhD thesis, ZeTeM, Faculty of Mathematics, University of Bremen, 2006.

[26] V. Nemchinski. Dross formation and heat transfer during plasma arc cutting. *J.Phys. D:Appl. Phys.*, **30**, 2566–2572, 1997.

[27] P. J. Ortoleva. *Geochemical Self-Organization. Oxford Monographs on Geology and Geophysics*, volume 23. Oxford University Press, NY, Oxford, 1994.

[28] V. G. Papadakis, C. G. Vayenas and M. N. Fardis. A reaction engineering approach to the problem of concrete carbonation. *AIChE Journal*, **35**(1639), 1989.

[29] A. Pawell. *Analytische und numerische Behandlung eines freien Randwertproblems zur Beschreibung der Reaktions-Diffusions-Kinetik von Beton.* PhD thesis, Bergakademie Freiberg, 1990.

[30] A. Pawell and K.-D. Krannich. Dissolution effects in transport in porous media. *SIAM J. Appl. Math.*, **1**, 89–118, 1996.

[31] D. Rosenthal. Mathematical theory of heat distribution during welding and cutting. *Welding Journal*, **20**, 220–234, 1941.

[32] L. I. Rubinstein. *The Stefan Problem*, volume 27. Translations of Mathematical Monographs, American Mathematical Society, 1971.

[33] A. Schmidt and A. Narimanyan. *Advanced numerical methods and their applications to industrial problems.* Summer school, Yerevan State University, 2004.

[34] A. Schmidt, M. Wolff and M. Böhm. Phase transitions and transformation-induced plasticity of steel in the framework of continuum mechanics. *J. Phys IV*, **120**, 145–152, 2004.

[35] A. Schmidt, M. Wolff, M. Böhm and G. L. Löwisch. Modelling and testing of transformation-induced plasticity and stress-dependent phase transformations in steel via simple experiments. *Computational Materials Science*, **32**, 604–610, 2005.

[36] W. Schulz, V. Kostrykin, H. Zefferer, D. Petring and R. Poprawe. A free boundary problem related to laser beam fusion cutting: Ode approximaton. *Int. J. Heat Mass Transfer*, **40**(12), 2913–2928, 1997.

[37] Z. Shen, S. Zhang, J. Lu and X. Ni. Mathematical modelling of laser induced heating and melting in solids. *Optics and Laser Technology*, **40**(8), 533–537, 2001.

[38] K. Sisomphon. *Influence of pozzolanic material additions on the development of the alkalinity and the carbonation behaviour of composite cement pastes and concretes.* Phd thesis, TU Hamburg-Harburg, 2004.

[39] M. Storti. Numerical modelling of ablation phenomena as two-phase Stefan problems. *Int.J.Heat Mass Transfer*, **38**(15), 2843–2854, 1995.

[40] B. An Ton. A Stefan-Signorini problem with set-valued mappings in domains with intersecting fixed and free boundarie. *Bollettino U.M.I.*, **7**, 231–249, 1994.